

# Molecular Dynamics Simulation of Organic Glass Formers: I. *ortho*-Terphenyl and 1,3,5-Tri- $\alpha$ -Naphthyl Benzene

JANE J. OU, SHAW H. CHEN

Materials Science Program, Chemical Engineering Department and Laboratory for Laser Energetics, Room 1213 COI, University of Rochester, 240 East River Road, Rochester, New York 14623-1212

Received 26 March 1997; accepted 15 August 1997

**ABSTRACT:** A computer code was prepared for the molecular dynamics (MD) simulation of a multimolecular system to atomic resolution. Based on a widely accepted force field and aided by simulated annealing of single molecules,  $\bar{V}$  and  $\bar{E}$  were computed for *ortho*-terphenyl and 1,3,5-tri- $\alpha$ -naphthyl benzene across an extended range of temperatures. Although neither the simulation time (40–100 ps) nor the system size (27 and 64 molecules) appeared to affect the computational results to an appreciable extent, it was clear that a longer simulation time or a larger system tended to yield a more consistent set of data. In comparison to experimental observations, simulation was capable of representing  $\bar{V}$  to within 2–7%,  $T_g$  to within 10 K, and  $\Delta C_p$  across  $T_g$  to within 10%. © 1998 John Wiley & Sons, Inc. *J Comput Chem* 19: 86–93 1998

**Keywords:** molecular dynamics simulation; *ortho*-terphenyl; 1,3,5-tri- $\alpha$ -naphthyl benzene

## Introduction

**M**aterials of all sorts of bonding characters (covalent, ionic, metallic, van der Waals,

Correspondence to: S. H. Chen; e-mail: shch@lle.rochester.edu  
Contract/grant sponsor: NSF; contract/grant number CTS-9500737

Contract/grant sponsor: U.S. Dept. of Energy; contract/grant number DE-FC03-92SF19460

and hydrogen bonding) are capable of glass formation via various methods including melt quenching, chemical and physical vapor deposition, and cold compression of crystals, to name just a few. Regardless of the material types and processing techniques, glass is characterized as a nonequilibrium material for which numerous theories have been formulated over the years.<sup>1–4</sup> Yet, the nature of glass transition is still being actively investi-

gated at present. "Why are certain materials more prone to glass formation than others?" and "What factors influence the morphological stability of glass against thermally activated recrystallization?" have remained the most challenging questions in glass science. Besides theories, molecular dynamics (MD) simulation has been advanced for the description of thermodynamic and transport properties across the glass transition temperature,  $T_g$ . Voluminous publications have appeared on the MD simulation of various materials ranging from monatomic<sup>5</sup> and molecular<sup>6</sup> to polymeric<sup>7</sup> systems modeled to differing levels of resolution. Despite the oft-quoted limitations (small sample size and short simulation time compared to laboratory experimentation on a real chemical system), glass transition phenomena of polymers have been simulated quite successfully following the united-atom approach.<sup>8,9</sup>

From an experimental perspective, a wealth of well-defined organic systems with low to medium molecular weights and varied morphological stabilities have been reported for potential applications to numerous advanced technologies.<sup>10–12</sup> From the standpoint of processing, materials capable of vitrification upon cooling without residual crystallinity are highly desirable. Attempts to relate glass-forming ability to chemical structure have not been as successful in view of the seemingly inconsistent molecular design rules that have been proposed on an empirical basis.<sup>11,13</sup> In the present work atomic-scale MD simulation of multimolecular systems was carried out as part of our continuing effort in the design, synthesis, and fundamental understanding of organic glass formers.<sup>14–16</sup> Specifically, the volumetric and thermal properties of glass-forming molecular materials were established as functions of temperature using a widely accepted force field. One obvious advantage of the atomic-scale modeling is the ease of implementation without introducing *ad hoc* parameters for a somewhat simplified molecular model. As our first attempt, *ortho*-terphenyl (*o*-TPh) and 1,3,5-tri- $\alpha$ -naphthyl benzene (T- $\alpha$ -NB) were selected for simulation. In contrast to laboratory experiments, MD simulation is limited to a very small system over an extremely short time scale, and hence an essentially infinitely fast cooling rate. The computational results validated against available experimental data<sup>17,18</sup> should permit a critical evaluation of MD simulation as a tool for molecular design.

## Simulation Method

The generic method formulated by Berendsen et al.<sup>19</sup> and applied by Picken et al.<sup>20</sup> to a nematic liquid crystalline compound was implemented in the present study for a system comprising  $m$  molecules, each consisting of  $n$  atoms, placed in a periodic box. The MD code was developed for implementation on a CRAY YMP2E/232 supercomputer. Key equations serving as the basis for simulation are laid out in the following. The potential energy,  $E_{\text{pot}}$ , of the system in the absence of bond stretching is expressed as<sup>21</sup>

$$E_{\text{pot}} = \frac{1}{2} \sum k_{\theta} (\theta - \theta_{\text{eq}})^2 + \frac{1}{2} \sum k_{\phi} [1 + \text{sign}(\text{per}) \cos(|\text{per}| \phi)] + \sum \varepsilon_{ij} \left[ \left( \frac{\sigma_{ij}}{r_{ij}} \right)^{12} - 2 \left( \frac{\sigma_{ij}}{r_{ij}} \right)^6 \right] + \frac{1}{2} \sum k_d d^2, \quad (1)$$

where  $\theta$ ,  $\phi$ ,  $r$ , and  $d$  represent bond angle, torsion angle, nonbonded distance, and out of plane distance, respectively. Alchemy III<sup>21</sup> provided an extensive compilation of empirically determined values for force constants  $k_{\theta}$ ,  $k_{\phi}$ ,  $k_d$ , periodicity (per) and the Lennard–Jones parameters  $\varepsilon$  and  $\sigma$ . Note that subscripts  $i$  and  $j$  represent atom to atom interactions of both intra- and intermolecular origins with  $r_{ij}$  denoting interatomic distance,  $\sigma_{ij} = \sigma_i + \sigma_j$ , and  $\varepsilon_{ij} = (\varepsilon_i \varepsilon_j)^{1/2}$ . Thus, in this work none of these parameters were adjusted to force an agreement between the computation and experiment.

A single molecule was constructed with all the bond lengths and bond angles at their equilibrium values: setting  $\theta = \theta_{\text{eq}}$  in eq. (1). The molecule was then allowed to undergo simulated annealing by randomly twisting dihedral angles.<sup>22</sup> A selected number of these molecules were placed in a box at a low density followed by an isotropic compression to a much higher density than the realistic value. The system was simulated at this density and constant temperature for 2 ps with a subsequent simulation at constant temperature and pressure for 100 ps, both involving coupling to an external bath.<sup>19</sup> Periodic boundary conditions were imposed throughout the simulation process. Based on  $E_{\text{pot}}$  as formulated in eq. (1), where  $\theta \neq \theta_{\text{eq}}$  in

general, for all atoms comprising the multimolecular system, the force  $\mathbf{F}_i$  on atom  $i$  was found using eq. (2):

$$\mathbf{F}_i = m_i \mathbf{a}_i = - \frac{\partial E_{\text{pot}}(\{\mathbf{r}\})}{\partial \mathbf{r}_i}, \quad (2)$$

which yielded the velocity,  $\mathbf{v}_i$ , and position,  $\mathbf{r}_i$ , of atom  $i$  via eqs. (3) and (4):

$$\mathbf{v}_i\left(t + \frac{\Delta t}{2}\right) = \mathbf{v}_i\left(t - \frac{\Delta t}{2}\right) + \frac{\mathbf{F}_i(t)\Delta t}{m_i}, \quad (3)$$

$$\mathbf{r}_i(t + \Delta t) = \mathbf{r}_i(t) + \mathbf{v}_i\left(t + \frac{\Delta t}{2}\right)\Delta t. \quad (4)$$

In eqs. (3) and (4)  $m_i$  is the mass of atom  $i$ ,  $t$  the simulation time, and  $\Delta t$  the length of a time step set at 2 fs in this work.

With  $\mathbf{r}_i$ ,  $\mathbf{v}_i$ , and  $\mathbf{F}_i$  for all atoms in the system determined via eqs. (1)–(4), the kinetic energy of the system,  $E_{\text{kin}}$ , was calculated using eq. (5),

$$E_{\text{kin}}\left(t - \frac{\Delta t}{2}\right) = \frac{1}{2} \sum m_i |\mathbf{v}_i|^2 \left(t - \frac{\Delta t}{2}\right), \quad (5)$$

from which the temperature,  $T$ , was determined using eq. (6),

$$T\left(t - \frac{\Delta t}{2}\right) = \frac{2 E_{\text{kin}}\left(t - \frac{\Delta t}{2}\right)}{\kappa(3N - M - 3)}. \quad (6)$$

In eq. (6)  $\kappa$  is the Boltzmann constant,  $N$  the total number of atoms, and  $M$  the number of constraints (i.e., the SHAKE<sup>23</sup> distance constraints) to keep the bond lengths at their equilibrium values. Furthermore, pressure in the  $k$  direction,  $P_k$ , was calculated with eq. (7):

$$P_k(t) = \frac{1}{3V(t)} \sum \left[ M_\alpha |\mathbf{V}_\alpha|^2 \left(t - \frac{\Delta t}{2}\right) - \sum \mathbf{R}_{\alpha\beta}(t) \cdot \mathbf{F}_{\alpha\beta}(t) \right], \quad (7)$$

where  $M_\alpha$  and  $\mathbf{V}_\alpha$  are the mass and the center of mass velocity of molecule  $\alpha$ , respectively,  $\mathbf{R}_{\alpha\beta}$  is the relative position vector of molecules  $\alpha$  and  $\beta$ ,  $\mathbf{F}_{\alpha\beta}$  is the sum of all pair interactions between molecules  $\alpha$  and  $\beta$ , and  $V$  is the volume of the simulation box. The temperature and pressure scaling of  $\mathbf{v}_i$  and  $S_k$ , the dimension of the simula-

tion box in the  $k$  direction, was accomplished through coupling to an external bath using the following formulas:

$$\mathbf{v}_i(t) \leftarrow \mathbf{v}_i(t) \left\{ 1 + 0.04 \left[ \frac{T_{\text{ref}}}{T(t)} - 1 \right] \right\}^{1/2}, \quad (8)$$

$$S_k(t) \leftarrow S_k(t) \left\{ 1 - 10^{-7} \left[ 1 - \frac{P_k(t)}{P_{\text{ref}}} \right] \right\}^{1/3} \quad (9)$$

in which  $P_{\text{ref}}$ , the reference pressure, was set at 1 atm, and  $T_{\text{ref}}$ , the reference temperature, was treated as an independent parameter in the simulation. For the present study the numerical coefficients in eqs. (8) and (9) were chosen to facilitate computation. The nonbonded cutoff was set at 8 Å, and a neighboring list for the nonbonded interactions was kept for the efficiency of computation and updated every 20 time steps.

In addition to the Alchemy III force field, the initial positions of all atoms in the system as well as initial dimensions of the simulation box were entered as input data. The temporal evolutions of  $S_k(t)$ ,  $P_k(t)$ ,  $E_{\text{pot}}(t)$  and  $E_{\text{kin}}(t)$  at 1 atm and  $T_{\text{ref}}$  emerged from the simulation process as described above, ultimately yielding the temporal evolutions of molar volume,  $\tilde{V}$ , and molar energy,  $\tilde{E}$ , defined as  $E_{\text{pot}} + E_{\text{kin}}$ . As the final step,  $\tilde{V}$  and  $\tilde{E}$  were time averaged to obtain equilibrium values.

## Results and Discussion

The force-field parameters pertaining to *o*-TPh and T- $\alpha$ -NB were assigned values selected from the Alchemy III data bank.<sup>21</sup> With all the bond angles and bond lengths adopting their equilibrium values, simulated annealing was conducted to produce conformations of single molecules as shown in Figure 1. The two “peripheral” phenyl rings make a 61° angle with the “central” phenyl ring in *o*-TPh. In T- $\alpha$ -NB the three naphthyl rings make an angle of  $90 \pm 2^\circ$  with the central phenyl ring. Note that these angles served as the initial conditions, and the equilibrium values would ultimately emerge from the MD simulation. As the first step in the simulation, 27 *o*-TPh molecules were evenly distributed in a box at a density of 0.59 g/cm<sup>3</sup> followed by compression at 300 K to a density of 1.60 g/cm<sup>3</sup>. Procedures as described earlier were followed to perform the simulation at discrete temperatures upon cooling from 340 K.

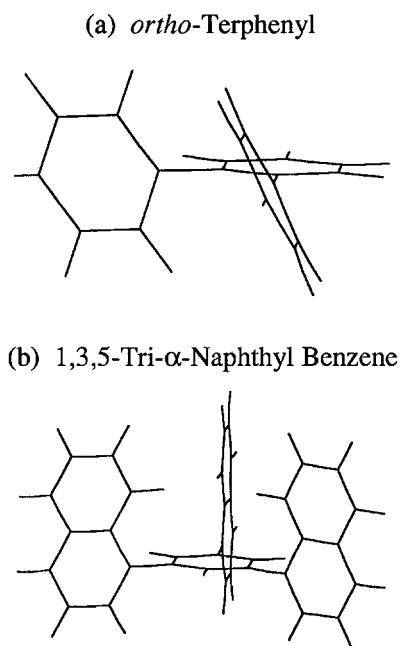


**FIGURE 1.** Conformation of a single molecule upon simulated annealing by randomly twisting dihedral angles while allowing all bond lengths and bond angles to adopt their equilibrium values: (a) *ortho*-terphenyl and (b) 1,3,5-tri- $\alpha$ -naphthyl benzene.

Two simulation runs for 40 and 80 ps each were performed at all temperatures to reveal the effect of simulation time. The value of  $\tilde{V}$  at a given temperature was determined by averaging all the data from the second half of the simulation time. The same simulation process was repeated for a system containing 64 molecules with an increased simulation time at lower temperatures.

The computed data for  $\tilde{V}$  under the specified conditions are shown in Figure 2. It is evident that a longer simulation time or a larger system yields a more consistent set of data. In particular, the following observations can be made: the simulated  $\tilde{V}$  seems to be rather insensitive to simulation time with an estimation over the experiment by 2–7%; a  $T_g$  is readily identified at the discontinuity in the slope of  $\tilde{V}$  versus  $T$ ; the 27- and 64-molecule system yields a  $T_g$  of 240 and 245 K, respectively, both in good agreement with the experimental value<sup>17</sup> of 243 K; and at temperatures below 290 K, the smaller system yields  $\tilde{V}$  closer to experimental observation. To address the last point, which is a little surprising, the temporal behavior of  $\tilde{V}$  for the two cases was examined. The raw data reproduced in Figure 3 indicate that the smaller system

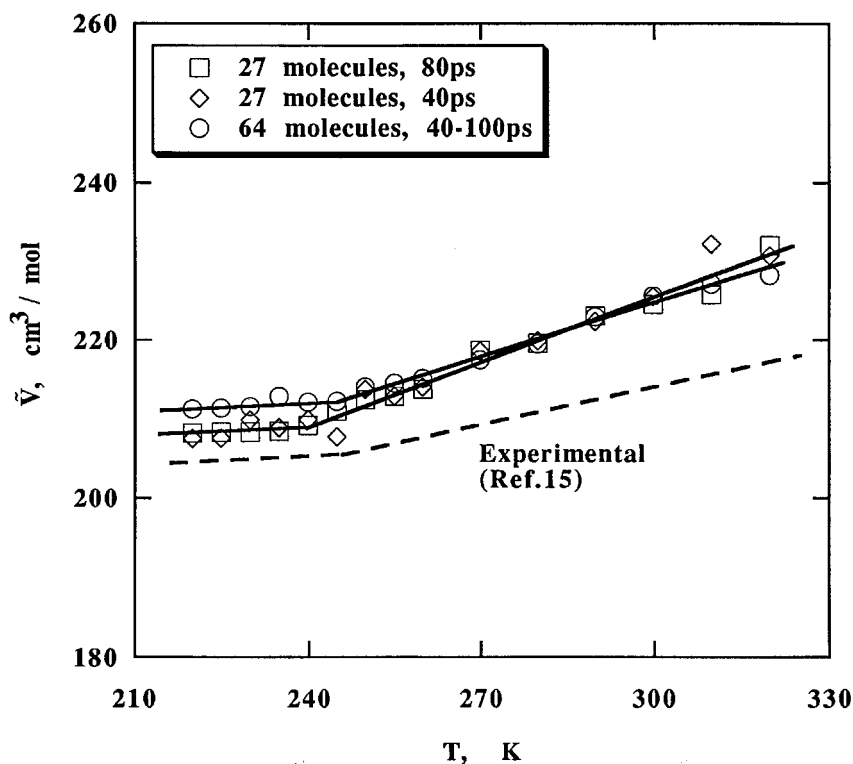


**FIGURE 2.** Computational results for  $\tilde{V}$  as a function of  $T$  in comparison to experimental data for *ortho*-terphenyl.

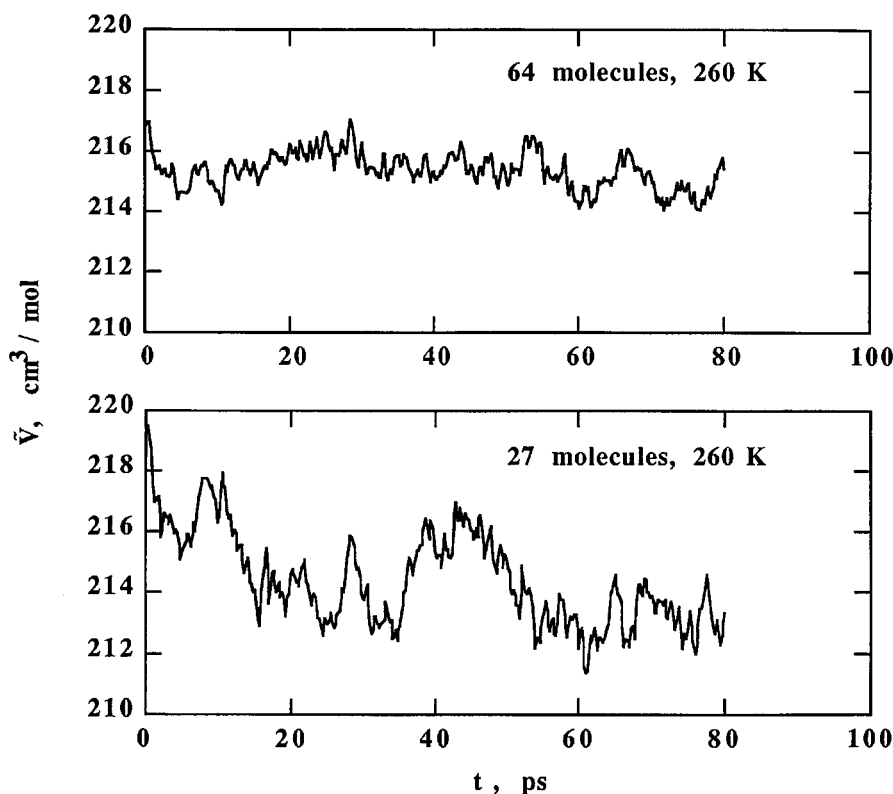


**FIGURE 3.** Computational results for  $\tilde{V}$  as a function of simulation time,  $t$ , for *ortho*-terphenyl.

undergoes a more pronounced fluctuation in volume during numerical simulation, thus allowing molecules to sample a greater number of individual conformations and configurations with respect to each other before settling into a more highly densely packed condition. Nevertheless, it should be remarked that temperature and molar volume were both found to be well equilibrated for the presently adopted system size within the allocated simulation time, as was also found by Picken et al. in the investigation of a nematic liquid crystal.<sup>20</sup>

To further assess the quantitative capability of the MD simulation,  $\tilde{E}$  as a function of  $T$  was computed for a system consisting of 27 molecules. The results obtained with 80-ps simulation time at each temperature are displayed in Figure 4. Across the entire temperature range two linear segments were identified, for which variances with the computed data points were calculated. The intersection of the two linear segments that gave the least variances of all combinations was identified as  $T_g$  at 240 K, a value in good agreement with the experiment. Validation of the computed data for  $\tilde{E}$  was not possible for lack of available experimental data. Generally, in condensed matters enthalpy is

literally equal to total energy, which had been verified in the present simulation. From the slopes of the two linear segments, the heat capacity,  $C_p$ , was found to be 125 and 152 cal/mol K across  $T_g$ . Compared to the reported experimental values of 55 and 85 cal/mol K,<sup>17</sup> the simulated data show a considerable deviation from the experiment. The overestimation of  $C_p$  can be attributed in part to the dependence of  $\tilde{E}_{\text{kin}}$  on  $T$ , determined to be 62 cal/mol K using eqs. (5) and (6). This value applies to both glassy and liquid phases. The balance of the computed  $C_p$  is contributed by  $\tilde{E}_{\text{pot}}$ , which undergoes a step change from 63 to 90 cal/mol K as the temperature is raised across  $T_g$ . Despite the disagreement with the experimentally observed  $C_p$  by a factor of 2, MD simulation is capable of producing a value for the step change in heat capacity,  $\Delta C_p$ , in fairly good agreement with the experiment, 27 versus 30 cal/mol K. Therefore, the presently implemented MD simulation is capable of representing  $\tilde{V}$ ,  $T_g$ , and  $\Delta C_p$  with reasonably good accuracy.

Another glass former, T- $\alpha$ -NB, was simulated to test the general applicability of the present MD approach. With bond angles and lengths assigned

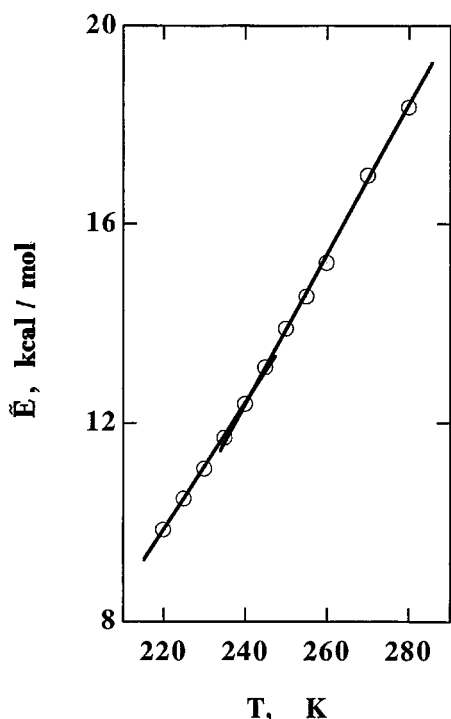
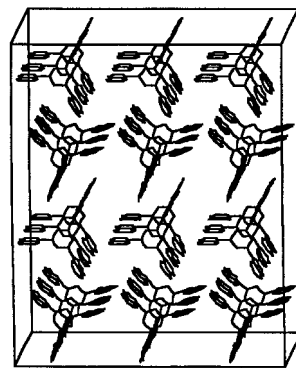


**FIGURE 4.** Computational results for  $\tilde{E}$  as a function of  $T$  for *ortho*-terphenyl.

their equilibrium values and with dihedral angles determined via simulated annealing, three, four, and three molecules were placed in the three dimensions of a periodic box, as shown in Figure 5a. The purpose for doing so, instead of selecting a cubic system (i.e., three molecules in all three directions), was to reach a relatively high initial density of 0.64 g/cm<sup>3</sup>, and hence a relatively low initial potential energy to facilitate computation. The system was then isotropically compressed at 500 K to a density of 1.40 g/cm<sup>3</sup>. A constant volume, constant temperature (500 K) simulation for 2 ps followed by a constant temperature (500 K), constant pressure (1 atm) simulation for 20 ps were performed before cooling to 450 K, where the system was simulated for 100 ps. Subsequently, a series of simulations were executed between 430 and 220 K for 70 ps at each temperature. The highly disordered state of molecules at all temperatures is as illustrated in Figure 5b for 315 K. The computed data for  $\tilde{V}$  and  $\tilde{E}$  as functions of temperature are plotted in Figure 6. The MD simulation was found to overestimate  $\tilde{V}$  by 1–7% across the entire temperature range covered by simulation, but no thermophysical data exist for a validation of the computed  $\tilde{E}$  or  $C_p$ . As in the case of *o*-TPh, the volumetric data show a higher degree

(a) Initial molecular arrangement



(b) Simulated arrangement at 315 K

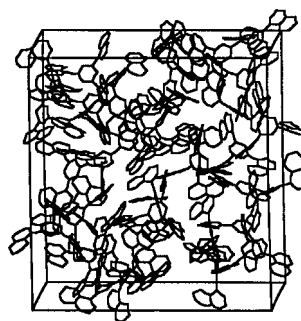


**FIGURE 5.** Snapshots of molecular arrangement during the MD simulation of 1,3,5-tri- $\alpha$ -naphthyl benzene: (a) initial condition and (b) “equilibrium” condition at 315 K.

of fluctuation around the two linear segments intersecting at  $T_g$  than the thermal data. On the other hand, the discontinuity in the slope of  $\tilde{V}$  versus  $T$  is more readily identifiable than the slope in  $\tilde{E}$  versus  $T$ . With respect to the plot of  $\tilde{E}$  versus  $T$ ,  $T_g$  was located following the same procedure as described above for *o*-TPh. The volumetric and thermal data reveal a  $T_g$  of 350 K, both in good agreement with the experimental observation of 342 K.<sup>18</sup>

## Summary

An MD simulation code was prepared for implementation on a multimolecular system modeled to atomic resolution. Two organic glass formers, *o*-TPh and Tri- $\alpha$ -NB, were selected for simulation to explore the capability and limitation of the present approach. Specifically, molar volume and energy as functions of temperature upon cooling across the glass transition temperature were ob-

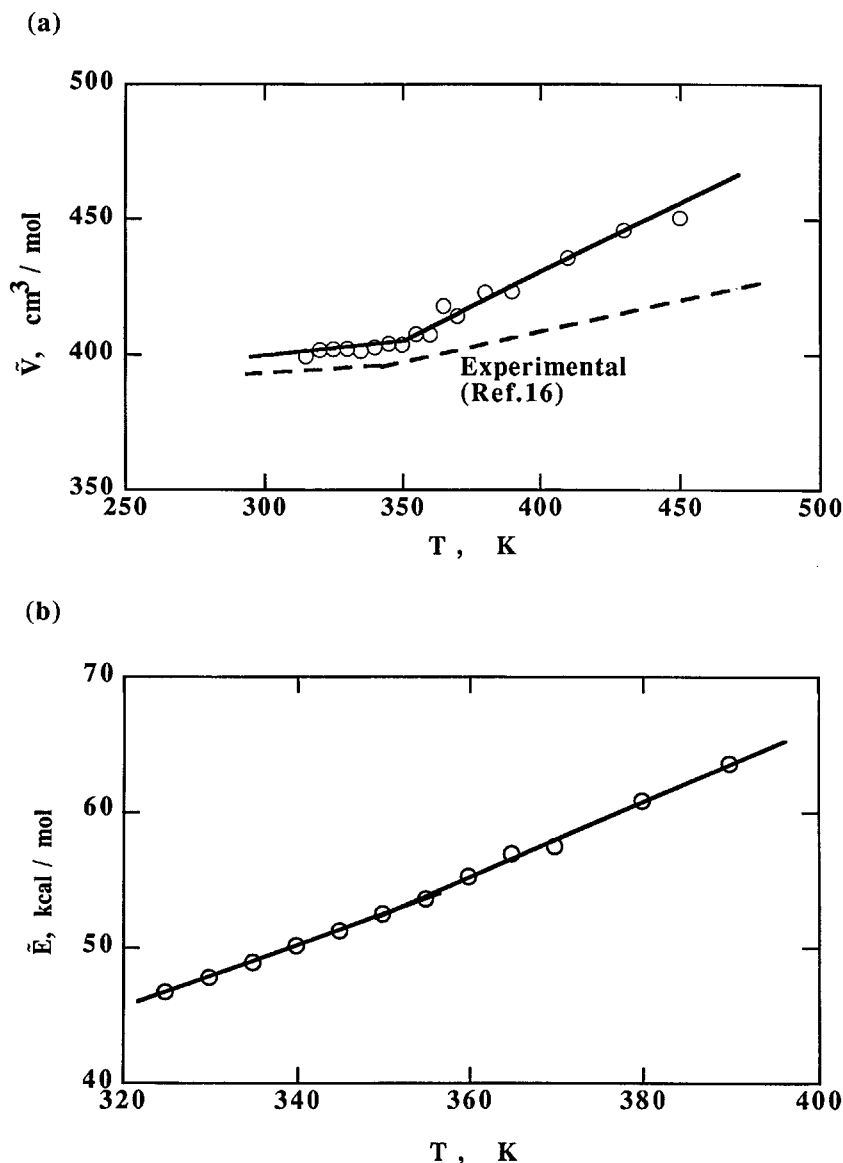


**FIGURE 6.** 1,3,5-Tri- $\alpha$ -naphthyl benzene computational results for (a)  $\tilde{V}$  as a function of  $T$  in comparison to experimental data and (b)  $\tilde{E}$  as a function of  $T$ .

tained using Alchemy III force field. The computed results were compared to relevant experimental data. The main points emerging from this study are summarized as follows:

1. The computational results are largely insensitive to simulation time in the range from 40 to 100 ps and to the number of molecules between 27 and 64. Nevertheless, it appears that a longer simulation time or a larger system yields a more consistent set of data.
2. The MD simulation overestimates molar volume by 2–7% with an error increasing with

temperature. No experimental data exist for a direct evaluation of the computed molar energy. In the case of *o*-TPh, simulation overestimates  $C_p$  by a factor of 2, but the computed  $\Delta C_p$  is fairly close to the experimental observation, 27 versus 30 cal/mol K.

3. The glass transition temperature is readily identified at the discontinuity in the slopes of the linear plots of molar volume and molar energy versus temperature. The resultant  $T_g$  values agree with experimental values to within 10 K. therefore, the presently implemented MD simulation seems to be capable

of predicting  $T_g$  to a satisfactory accuracy as an important material property.

## Acknowledgment

This work was performed as a part of our advanced organic materials research supported by the U.S. National Science Foundation (CTS-9500737), the Japanese Ministry of International Trade and Industry, and the U.S. Department of Energy, Office of Inertial Confinement Fusion, under Cooperative Agreement DE-FC03-92SF19460, the University of Rochester. In particular, the authors acknowledge access to the supercomputing facilities made available by the Theory Division of the Laboratory for Laser Energetics.

## References

1. W. Götze and L. Sjögren, *Rep. Prog. Phys.*, **55**, 241 (1992).
2. S. V. Nemilov, *Thermodynamic and Kinetic Aspects of the Vitreous State*, CRC Press, Boca Raton, Florida (1995).
3. S. R. Elliott, *Physics of Amorphous Materials*, 2nd ed., Longman Group UK Limited, Essex, U.K, 1990.
4. C. A. Angell, *Science*, **267**, 1924 (1995).
5. J. R. Fox and H. C. Andersen, *J. Phys. Chem.*, **88**, 4019 (1984).
6. J. L. Lewis and G. Wahnström, *Phys. Rev. E*, **50**, 3865 (1994).
7. L. Monnerie and U. W. Suter, *Atomistic Modeling of Physical Properties, Advances in Polymer Science*, Vol. 116, Springer-Verlag, Berlin, 1994.
8. D. Rigby and R.-J. Roe, *J. Chem. Phys.*, **87**, 7285 (1987).
9. J. Han, R. H. Gee, and R. H. Boyd, *Macromolecules*, **27**, 7781 (1994).
10. P. M. Lundquist, R. Wortmann, C. Geletneky, R. J. Twieg, M. Jurich, V. Y. Lee, C. R. Moylan, and D. M. Burland, *Science*, **274**, 1182 (1996).
11. K. Naito and A. Miura, *J. Phys. Chem.*, **97**, 6240 (1993).
12. S. H. Chen, H. Shi, B. M. Conger, J. C. Mastrangelo, and T. Tsutsui, *Adv. Mater.*, **8**, 998 (1996).
13. W. Wedler, D. Demus, H. Zschke, K. Mohr, W. Schäfer, and W. Weissflog, *J. Mater. Chem.*, **1**, 347 (1991).
14. S. H. Chen, J. C. Mastrangelo, H. Shi, A. Bashir-Hashemi, J. Li, and N. Gelber, *Macromolecules*, **28**, 7775 (1995).
15. J. C. Mastrangelo, B. M. Conger, S. H. Chen, and A. Bashir-Hashemi, *Chem. Mater.*, **9**, 227 (1997).
16. S. H. Chen, J. C. Mastrangelo, T. N. Blanton, and A. Bashir-Hashemi, *Macromolecules*, **30**, 93 (1997).
17. R. J. Greet and D. Turnbull, *J. Chem. Phys.*, **46**, 1243 (1967).
18. D. J. Plazek and J. H. Magill, *J. Chem. Phys.*, **45**, 3038 (1966).
19. H. J. C. Berendsen, J. P. M. Postma, W. F. van Gunsteren, A. DiNola, and J. R. Haak, *J. Chem. Phys.*, **81**, 3684 (1984).
20. S. J. Picken, W. F. van Gunsteren, P. Th. van Duijnen, and W. H. de Jeu, *Liq. Cryst.*, **6**, 357 (1989).
21. Alchemy III, Tripos Associates, Inc. (1992).
22. S. R. Wilson and W. Cui, *Biopolymers*, **29**, 225(1990).
23. J. P. Ryckaert, G. Ciccotti, and H. J. C. Berendsen, *J. Comput. Phys.*, **23**, 327 (1977).